Reprinted from **APPLIED OPTICS**, Vol. 9, page 1192, May 1970

Degenerate Optical Cavities. III: Effect of Aberrations

J. A. Arnaud

The capability of degenerate optical cavities to transmit faithfully incident optical signals with arbitrary wavefronts is limited primarily by geometrical optics aberrations. This capability is expressed by an acceptance factor which is calculated for various types of cavities lacking first-order degeneracy, or suffering from primary aberrations. It is found that the acceptance factors of spherically symmetric cavities are larger, by orders of magnitude, than the acceptance factors of cavities possessing only rotational symmetry (such as the well-known confocal cavity). The correction of primary aberrations for both types of cavities is discussed. Acceptance factors of the order of 10^7 with finesses of the order of 100 can be obtained. The mechanical accuracy required is, however, a few orders of magnitude higher than in conventional optical instruments.

I. Introduction

The first-order properties of degenerate optical cavities, defined as optical systems where all the ray trajectories are closed curves of equal optical length, have been discussed in previous papers.[1,2] It has also been pointed out[1] that the degeneracy condition is met exactly in a few continuously varying refractive index media, such as the well-known Maxwell fisheye medium.[3] The configurations usually encountered, which employ homogeneous materials, suffer, however, from various types of aberrations which limit their performances.

These limitations must be discussed in relation to the specific applications considered, which are essentially of two types. In one type of application, offset paths are selected inside the cavity with the help of one or two small apertures (or equivalent electrooptic components, as in the scan laser[4]). As a result of the cavity degeneracy, the diffraction losses resulting from the apertures are not affected by moderate path offsets. The presence of aberrations in the cavity, however, does increase the diffraction losses, for large offsets, and modifies the resonant frequencies.

We are mainly concerned in this paper with a second type of application: the measurement of the frequency spectrum of extended incoherent sources (or of sources of unknown field distribution). The most commonly used scanning interferometer is, at the present time, the plane parallel Fabry-Perot. This is a mode-degenerate cavity[1] which offers an unlimited acceptance area but only a very small acceptance angle. It was shown by Connes[5] in 1956 that a confocal cavity incorporating two spherical mirrors is generally superior to the plane parallel configuration, in terms of étendue resolution product. This confocal cavity is half-degenerate, in the sense that it takes a ray two round trips to retrace its path.[1] This peculiarity introduces limitations which were discussed before.[1,5] It is shown in this paper that truly degenerate cavities possessing spherical symmetry, such as the concentric cavity proposed by Pole,[6] exhibit étendue resolution products which are higher, by orders of magnitude, than those of confocal cavities. The étendue of these cavities can be further increased by correcting the primary spherical aberration. Degenerate cavities possessing only rotational symmetry are of interest in many applications; they are also investigated.

The transmission of aberrated degenerate cavities is calculated by adding the fields of successive passes. In a first step the phase distortion introduced on the field of an incident wave is evaluated for one round trip in the cavity, according to the laws of geometrical optics by both analytical and ray tracing methods. Because the aberrations are small in the region of interest, the fields of the successive passes form a geometrical series which can be summed up. The rest of the calculation consists of integrating the power within the limits of the cavity apertures. The splitting of mode frequencies, resulting from edge diffraction at internal apertures, is neglected. This approximation is permissible for cavities whose Fresnel's numbers are much larger than the finesse. When this condition is not satisfied, one implicitly assumes that the apertures are located between the cavity and the detector, rather than inside the cavity.

The limitations in the use of degenerate optical cavities as scanning interferometers are essentially of a practical nature (accuracy). They are emphasized in the conclusion.

The author is with the Bell Telephone Laboratories, Inc., Crawford Hill Laboratory, Holmdel, New Jersey 07733.
Received 13 October 1969.

II. General Results

The capability of optical systems of transmitting optical beams of large transverse extent and originating from various directions in space can be expressed by a dimensionless acceptance factor N defined by[7]

$$N = P/\lambda^2\mathcal{B}, \tag{1}$$

where P is the power transmitted by the system for an extended lambertian source of luminance $\mathcal{B}$ and wavelength λ. For a resonant system, the source is required to be quasimonochromatic; it can be obtained, for instance, by illuminating a rotating diffusing plate with a laser.* The function $N(\nu)$, where ν is the optical frequency, is generally broader than the resonance curve obtained with a coherent beam. A quantity called *étendue*, approximately equal to $N\lambda^2$, is sometimes used in place of the acceptance factor. The acceptance factor of systems resonating on a single mode is unity.

As is well known, an extended lambertian source can be represented either by a surface whose elementary areas $d\sigma$ radiate independently with intensity patterns

$$\mathcal{B}\cos\alpha d\sigma, \tag{2}$$

α being the angle with the normal to the surface, or by a uniform spectrum of plane waves with power densities

$$\mathcal{B}d\Omega, \tag{3}$$

for an elementary solid angle $d\Omega$. A Luneburg lens of large radius[3] provides a concrete way of transforming the plane waves (within $d\Omega$) of the plane wave representation into the point sources (within $d\sigma$) of the point source representation. Locally, the transformation from Eq. (3) to Eq. (2) is based on the sine law, applicable to any aplanatic system.[3]

Reciprocity laws show that the acceptance factor of a system does not change when the source and the detector positions are exchanged. In addition, as a result of the invariance of the luminance of extended lambertian sources through lossless media,[8] it is not affected by the introduction of lossless elements on either side. It is often of interest to trade the acceptance angle for the acceptance area or vice versa, the product of these two quantities (étendue) staying constant. In the case of a plane parallel Fabry-Perot, for instance, the acceptance angle can be increased at the expense of the acceptance area (which is, in principle, unlimited) with the help of an inverted telescope.

A. Acceptance Factor of Cavities Free of Aberration

The acceptance factor of degenerate cavities free of aberration, but incorporating a number of apertures of large dimensions, can be readily evaluated. Let us assume that the losses are negligible and that the end mirrors have equal reflectivity. Since any ray retraces its own path after a round trip in the cavity, it is sufficient to determine what rays originating from the source make a round trip without being intercepted by a stop. Following a procedure used in conventional optical instruments, we calculate the image of each stop back into the object space. For a linear cavity, however, stops whose location does not coincide with the end mirrors must be considered twice, as they are crossed twice by the optical axis in a round trip. As an example, let us consider the degenerate cavity shown in Fig. 1(a), which incorporates two identical confocal lenses of focal length f between two plane end mirrors, and a single coaxial circular stop, of radius R, adjacent to one of the two lenses. The two images of this stop in the object space are shown in Fig. 1(b). The acceptance factor of such a system, consisting of two coaxial circular apertures of equal radius R, separated by a distance $d = 2f$, is known to be[7]

$$N = (\pi^2/2\lambda^2)[d^2 + 2R^2 - (d^4 + 4d^2R^2)^{\frac{1}{2}}], \tag{4a}$$

or

$$N \simeq \pi^2R^4/\lambda^2(2f)^2, \tag{4b}$$

if f is much larger than R. Within the present approximations, the resolution is not affected by stops in the cavity. This conclusion applies, in particular, to the Maxwell fisheye cavity described in Ref. 1 which incorporates a reflecting sphere of radius R. The acceptance factor of such a cavity, which is equivalent to a single aperture of radius R, is obtained by setting $d = 0$ in Eq. (4a). One obtains

$$N = \pi^2(R/\lambda)^2. \tag{5}$$

Equation (5) shows that the acceptance factor may be as high as 10^9 at a wavelength of 10 μm, for a cavity radius of 10 cm. In Secs. II.B and II.C, we evaluate the reduction in acceptance factor, with respect to this optimum value, which results from geometrical optics aberrations.

B. Methods of Calculation of the Round Trip Wave Aberration

Let us choose an arbitrary reference plane in the cavity, and a point source x_0, y_0 in that plane, which generates a spherical wavefront (see Fig. 2). For simplicity, one assumes that the refractive index is unity at that plane. At a large distance from the source, the difference between the wavefront transformed after a round trip in the system, and the original spherical wavefront (henceforth called *wave difference*) is given, in a direction defined by direction cosines p_1 and q_1, by

$$\Delta(x_0,y_0,p_1,q_1) = \overline{AQ'} = \overline{AQ} + \overline{QQ'} \equiv W(x_0,y_0,p_1,q_1) + x_0p_1 + y_0q_1, \tag{6}$$

where Q and Q' are the feet of the perpendiculars drawn on the output ray from, respectively, the origin and the point source. The upper bars in Eq. (6) indicate optical distances, and $W(x_0,y_0,p_1,q_1)$ denotes the mixed characteristic function of the optical system. Let us now expand Δ in series of its arguments:

$$\Delta = L + \Delta^{(1)} + \Delta^{(2)} + \Delta^{(3)} + \Delta^{(4)} + \Delta^{(5)} + \Delta^{(6)} + \ldots. \tag{7}$$

L is the round trip path length of the optical axis and $\Delta^{(m)}$ is a polynomium of degree m in x_0, y_0, p_1, and q_1. $\Delta^{(1)}$ expresses a misalignment of the cavity and $\Delta^{(2)}$ a lack of first-order degeneracy. We are mainly concerned with the third- and fifth-order aberration terms, denoted here $\Delta^{(4)}$ and $\Delta^{(6)}$, respectively. The terms $\Delta^{(3)}$ and $\Delta^{(5)}$ appear only in the case of cavities lacking rotational symmetry.

There are various ways of calculating the wave difference Δ. Ray tracing methods give the exact path length U of a ray (defined at the input plane by x_0, y_0, p_0, q_0) from the reference plane to the point x_1, y_1 where it crosses again the reference plane after a round trip. Δ is related to U by

$$\Delta = U - [p_1(x_1 - x_0) + q_1(y_1 - y_0)]. \tag{8}$$

Let us consider a system with rotational symmetry, and suppose that the function $U(p_1)$ at $x_0 = y_0 = 0$ is known. From Eq. (6), and $x_1 = -\partial W/\partial p_1$ (see Ref. 3), one easily finds that

$$\Delta(p_1) = L - p_1\int_0^{p_1}\frac{U(p_1) - L}{p_1^2}\,dp_1. \tag{9}$$

Equation (9) leads to the following relations:

$$\Delta^{(2)}(p_1) = -U^{(2)}(p_1), \tag{9a}$$

$$\Delta^{(4)}(p_1) = -\tfrac{1}{3}U^{(4)}(p_1), \tag{9b}$$

$$\Delta^{(6)}(p_1) = -\tfrac{1}{5}U^{(6)}(p_1), \tag{9c}$$

which are useful in the case of cavities with spherical symmetry, because $U(p_0)$ can be evaluated exactly, if the input mirror is taken as a reference surface. A detailed analysis shows that for a cavity close to degeneracy and $m > 2$, p_1 can be replaced by p_0 in the expression of U, and that Eqs. (9b) and (9c) are unchanged (for axial sources) if the reference surface is curved, rather than plane.

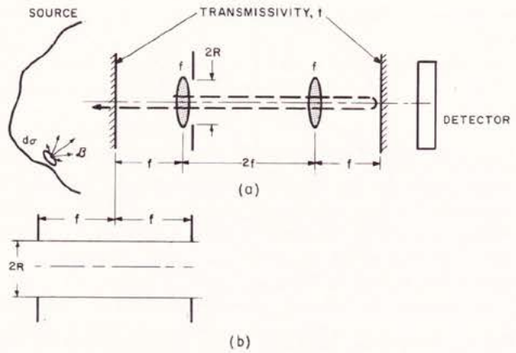

Fig. 1. (a) represents a degenerate cavity incorporating one internal stop. Its two images in the object space, taken along the folded optical axis (dotted line), are shown in (b).

Fermat's principle shows that primary aberrations can alternately be obtained by evaluating the optical length of quasiparaxial rays, i.e., closed paths whose slope discontinuities are located at the refractive or reflecting surfaces, but which assume slopes or positions given by the paraxial approximation. This method will be used for cavities possessing rotational symmetry.

C. Multipath Systems

Let $\mathcal{L} = 1 - t$ denote the field round trip loss of the cavity, t being the power transmissivity of both the input and output mirrors. The finesse of the cavity would be[2]

$$\mathfrak{F}_0 = \pi(1 - \mathcal{L})^{-1} = \pi t^{-1}, \tag{10}$$

if there were no aberration and if $t^{-1} \gg 1$.

Under the conditions that both $\mathfrak{F}_0$ and N are much larger than unity, one finds that the intensity variations resulting from the phase distortions are negligible in the domain of x_0, y_0, p_1, q_1 of interest. In addition, since a ray nearly retraces its own path after a round trip, the total phase distortion is proportional to the number of round trips in the cavity. Using these approximations, the total field in the cavity resulting from an elementary lambertian source of luminance $\mathcal{B}$, located at x_0, y_0 with a normal directed along the z axis and an area $d\sigma$, is given by a geometrical series

$$E_T = t^{\frac{1}{2}}(\mathcal{B}\cos\alpha d\sigma)^{\frac{1}{2}}\sum_{n=0}^{\infty}\mathcal{L}^n\exp[-jkn\Delta(x_0,y_0,p_1,q_1)]$$
$$= (t\mathcal{B}\cos\alpha d\sigma)^{\frac{1}{2}}\{1 - \mathcal{L}\exp[-jk\Delta(x_0,y_0,p_1,q_1)]\}^{-1}. \tag{11}$$

The acceptance factor, according to Eq. (1), is obtained by integrating $|E_T|^2$ over all directions p_1, q_1, with an elementary solid angle $d\Omega = dp_1dq_1(\cos\alpha)^{-1}$ and over the surface S of the source. The result is multiplied by t, to obtain the total output power, and divided by $\mathcal{B}\lambda^2$. We get, also using Eq. (10),

$$N = \lambda^{-2}\iint_S d\sigma\iint_\Omega\frac{dp_1dq_1}{1 + (2\mathfrak{F}_0/\pi)^2\sin^2[\frac{1}{2}k\Delta(x_0,y_0,p_1,q_1)]}. \tag{12}$$

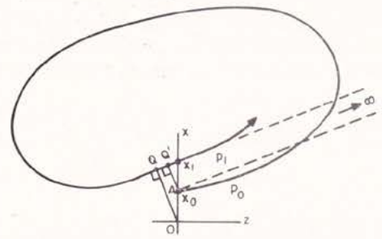

Fig. 2. This figure represents schematically a ring type cavity. The round trip mixed characteristic is defined as the optical length $\overline{AQ}$. The difference between the wavefront after a round trip and the original spherical wavefront originating from A, is, at infinity, in the direction p_1, the optical length $\overline{AQ'}$.

* Alternately, one may use a coherent monochromatic source with a narrow radiation pattern, whose axis is offset and rotated about a fixed point, and take the average of P over all offsets and rotation angles.

This result can alternately be obtained from the plane wave representation of extended sources.

Equation (12) shows that if there were no apertures in the cavity to bound the area S and the solid angle Ω, N would be nearly independent of the frequency and all resolution would be lost. If, on the other hand, very small apertures were introduced to select a narrow pencil, only a small portion of the incident power would be transmitted to the detector. It is generally possible, however, to introduce apertures which eliminate the outer rings of interference [corresponding to arguments of the sine function, in Eq. (12), close to $2K\pi$, K being a positive integer] without affecting the central zone (corresponding to $K = 0$); this is assumed henceforth. In the neighborhood of a resonance ($k = k_0$), we have

$$\sin\tfrac{1}{2}k\Delta = \sin\tfrac{1}{2}k[L + (\Delta - L)] \simeq (k - k_0)L/2 + (k/2)(\Delta - L), \tag{13}$$

and Eq. (12) becomes, for a frequency offset $\Delta\nu$,

$$N = \lambda^{-2}\iint_S d\sigma \iint_\Omega \frac{dp_1dq_1}{1 + (2\mathfrak{F}_0L/\lambda)^2[(\Delta\nu/\nu) + \Delta^{(m)}L^{-1}]^2}, \tag{14}$$

where only one order (m) of wave aberration is considered. The acceptance factor, as given by Eq. (14), is evaluated in the next sections for simple degenerate cavities possessing spherical or rotational symmetry.

III. Spherical Cavities

Spherical cavities are optical systems where the refractive and reflective surfaces are portions of concentric spheres. A typical spherical cavity is represented in Fig. 3. It incorporates an internal spherical lens which images a point A of one end mirror into the point B of the other end mirror which is aligned with the system center C. It is obvious that, if the imaging were sharp the cavity would be free of aberration. This result can be achieved, in principle, with a Luneburg lens.* In the following sections we consider the effect of first-, third-, and fifth-order aberrations. To preserve the resolution, a stop is introduced as shown in Fig. 3, with such a radius that it transmits only the central zone, as discussed in Sec. II. C.

A. Lack of Exact First-Order Degeneracy

Let R denote the radius of the input mirror, taken as the reference surface. By specifying that any ray going through the cavity center retraces its own path, one finds that the cavity ray matrix has the form

$$\begin{bmatrix} x_1 \\ p_1 \end{bmatrix} \equiv \begin{bmatrix} A & B \\ C & D \end{bmatrix}\begin{bmatrix} x_0 \\ p_0 \end{bmatrix} \quad \begin{bmatrix} 1 - B/R & B \\ -B/R^2 & 1 + B/R \end{bmatrix}\begin{bmatrix} x_0 \\ p_0 \end{bmatrix}, \tag{15}$$

* Such a Luneburg lens cavity[1] has the remarkable property of giving a perfect *real* image of a homogeneous volume. The image space coincides with the object space. It is easy, however, if desired, to separate the image space from the object space with the help of a plane mirror. There is apparently no other known optical system possessing such a property.

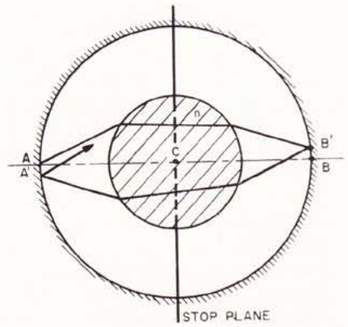

Fig. 3. The primary aberrations of the lens incorporated in this concentric cavity can be corrected by an aspheric plate (dotted line) similar to the one used in Schmidt cameras, or, preferably, with a concentric shell as shown in Fig. 6. The aperture is aimed at selecting the central zone, in order to preserve the cavity resolution.

with $B \ll R$. Notice that $A + D = 2$, spherical cavities being always mode-degenerate.[1] They lack first-order degeneracy, however, if $B \neq 0$. Within the paraxial approximation, the wave aberration is

$$\Delta^{(2)}(x_0,p_1) = (C/2D)x_0^2 - (B/2D)p_1^2 + (1 - D^{-1})x_0p_1. \tag{16}$$

Introducing in Eq. (16) the values of B, C, D given by Eq. (15), one has, at $x_0 = 0$,

$$\Delta^{(2)}(p_1) = -[(B/2)(1 + B/R)]p_1^2 \simeq -Bp_1^2/2. \tag{17}$$

Introducing Eq. (17) in Eq. (14), one finds an acceptance factor,

$$N = (\pi S/\lambda B)\mathfrak{F}_0^{-1}[\tan^{-1}(\mathfrak{a} - \delta) + \tan^{-1}(\delta)], \tag{18}$$

where the area S of the source is assumed to be much smaller than $2\pi R^2$, and where

$$\delta \equiv (2\mathfrak{F}_0L/\lambda)(\Delta\nu/\nu) \tag{19}$$

is proportional to the relative frequency offset $\Delta\nu/\nu$. $\mathfrak{a}$ is an aperture factor, defined by

$$\mathfrak{a} \equiv (B\mathfrak{F}_0/\lambda)p_{\max}^2, \tag{20}$$

where $p_{\max}$ is the maximum allowed angle, as defined by the aperture radius. The frequency dependance of N, normalized to unity for $\delta = 0$, is plotted in Fig. 4, for $\mathfrak{a} = 1$ (curve b). This is a symmetrical but offset function of δ. For $\mathfrak{a} = 1$, the resolution is about 15% lower than for small apertures, and the acceptance factor is half the value reached for large apertures.

The acceptance factor of a plane parallel Fabry-Perot, of area S, considered as a spherical cavity in the limit where $R \to \infty$, is obtained by setting $B = 2d$ in Eq. (18), d being the mirror spacing. Equation (18) becomes, for $\mathfrak{a} = 1$, at the peak of the response curve ($\delta = 0.5$),

$$N = 1.48(S/\lambda d)\mathfrak{F}_0^{-1}. \tag{21}$$

This expression is also readily obtained from the plane wave representation of lambertian sources.

Let us make the following numerical example: $\mathfrak{F}_0 = 100$, $\lambda = 10\ \mu$m, $S = 10$ cm^2, and $d = 1$ cm. One finds, from Eq. (21), $N = 148$. From Eq. (20), the acceptance angle is $p_{\max} = 2.2 \times 10^{-3}$.

B. Concentric Cavity

Let us now assume that the condition for first-order degeneracy is fulfilled ($B = 0$), and calculate the effect of spherical aberration on a degenerate cavity incorporating a spherical lens of refractive index n and radius r in a concentric reflecting sphere of radius R. The round trip path length is easily obtained from the Bouguer formula.[11] Taking the input mirror as a reference surface as before, we have

$$\begin{aligned} U(p_0)/4R &= (1 - p_0^2)^{\frac{1}{2}} + n\frac{r}{R}\left(1 - \frac{p_0^2R^2}{n^2r^2}\right)^{\frac{1}{2}} - \frac{r}{R}\left(1 - \frac{p_0^2R^2}{r^2}\right)^{\frac{1}{2}} \\ &\simeq \left(1 - \frac{r}{R} + n\frac{r}{R}\right) - \frac{p^2}{2}\left[1 + \frac{R}{r}\left(\frac{1}{n} - 1\right)\right] - \frac{p^4}{8} \\ &\times \left[1 + \frac{R^3}{r^3}\left(\frac{1}{n^3} - 1\right)\right] + \ldots \equiv [L + U^{(2)} + U^{(4)} \\ &+ \ldots]/4R, \end{aligned} \tag{22}$$

where $p_0 \simeq p_1 \equiv p$ is the input ray direction cosine.

The condition for first-order imaging of opposite points of the reflecting sphere [$U^{(2)} = 0$] is, from Eq. (22),

$$r = [(n - 1)/n]R, \tag{23}$$

and the third-order wave aberration for a round trip is, from Eqs. (9b), (22), and (23),

$$\Delta^{(4)} = -(p^4/2)[n/(n - 1)^2]R. \tag{24}$$

Ray tracing* shows that higher order terms do not exceed 7% of $\Delta^{(4)}$ when $p < 0.1$. The integration over p_1 and q_1 in Eq. (14) can be taken from $-\infty$ to $+\infty$ with a negligible error. Let us take the source as coincident with the input half sphere of area $2\pi R^2$. Substituting $\Delta^{(4)}$ from Eq. (24) into Eq. (14), one obtains an acceptance factor,

$$N = \pi^3 2^{-\frac{1}{2}}(R/\lambda)^{3\frac{1}{2}}\mathfrak{F}_0^{-\frac{1}{2}}(n - 1)n^{-\frac{1}{2}}H(\delta), \tag{25a}$$

where

$$H(\delta) \equiv [(1 + \delta^2)^{-\frac{1}{2}} - \delta(1 + \delta^2)^{-1}]^{\frac{1}{2}}. \tag{25b}$$

δ is a quantity proportional to the frequency offset, which was defined before in Eq. (19). The function $H(\delta)$ is plotted in Fig. 4 (curve c). One notices that $H(\delta)$ decreases only slowly when the source frequency is increased above the resonant frequency ($\delta > 0$). The reason is that for frequencies higher than the resonant frequency the central zone simply transforms into a ring of increasing diameter. A better resolution is obtained, as shown by Hercher,[9] with apertures smaller than the one presently considered (which is only aimed at separating the central zone from the outer rings). Equation (25a) shows that the acceptance factor of the cavity increases with its dimensions as $(R/\lambda)^{3\frac{1}{2}}$. N also increases with the refractive index n.

For $n = 4$ (germanium), $\mathfrak{F}_0 = 100$, $R = 10$ cm, and $\lambda = 10\ \mu$m, the maximum acceptance factor, as given by Eqs. (25a) and (25b), is $N = 3.8 \times 10^6$.

One way of correcting the spherical aberration of the internal lens consists of introducing an aspherical plate at the cavity center as shown by a dotted line in Fig. 3. This plate, similar to the one used in the Schmidt camera, would free the cavity from primary aberrations, but the acceptance area would be restricted by higher order aberrations. A different method of correction is discussed in Sec. III.C.

* The ray tracing programs used in the present work are written in superbasic with double precision (16 decimals).

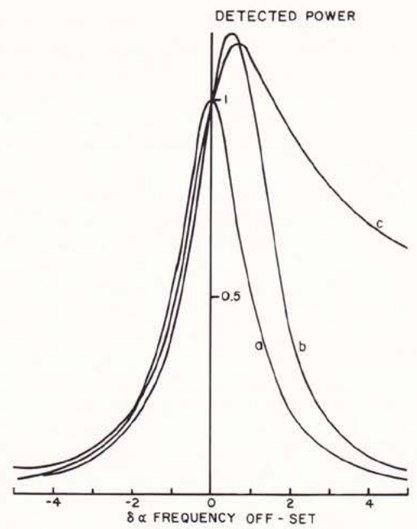

Fig. 4. (a) Normalized transmission vs frequency curves of aberrationless cavities (b), cavities suffering from lack of first-order degeneracy and (c), cavities suffering from spherical aberration.

C. Corrected Concentric Cavity

The possibility of correcting the spherical aberration of a spherical lens with the help of a concentric spherical shell of refractive index n' and radius $r' > r$ is investigated in in this section. The path length $U(p)$ becomes[11]

$$\begin{aligned} \frac{U(p)}{4R} &\simeq (1 - p^2)^{\frac{1}{2}} + n'\frac{r'}{R}\left(1 - \frac{p^2R^2}{n'^2r'^2}\right)^{\frac{1}{2}} - \frac{r'}{R}\left(1 - \frac{p^2R^2}{r'^2}\right)^{\frac{1}{2}} \\ &+ n\frac{r}{R}\left(1 - \frac{p^2R^2}{n^2r^2}\right)^{\frac{1}{2}} - n'\frac{r}{R}\left(1 - \frac{p^2R^2}{n'^2r^2}\right)^{\frac{1}{2}} = \left(1 - \frac{r'}{R}\right) \\ &+ n'\left(\frac{r'}{R} - \frac{r}{R}\right) + n\frac{r}{R} - \frac{p^2}{2}\left[1 + \frac{R}{r'}\left(\frac{1}{n'} - 1\right) + \frac{R}{r}\right. \\ &\times \left.\left(\frac{1}{n} - \frac{1}{n'}\right)\right] - \frac{p^4}{8}\left[1 + \frac{R^2}{r'^2}\left(\frac{1}{n'^2} - 1\right) + \frac{R^2}{r^2}\left(\frac{1}{n^2} - \frac{1}{n'^2}\right)\right] \\ &- \frac{p^6}{16}\left[1 + \frac{R^5}{r'^5}\left(\frac{1}{n'^5} - 1\right) + \frac{R^5}{r^5}\left(\frac{1}{n^5} - \frac{1}{n'^5}\right)\right] + \ldots. \end{aligned} \tag{26}$$

Numerical calculations show that the second and third terms in the expansion of Eq. (26) can be made equal to zero simultaneously, if $n' > n$. The primary spherical aberration can consequently be made to vanish. Notice that, when $n' > n$, the core has a convergent effect which overcomes the divergent effect due to the shell. The fifth-order spherical aberration, reaches a minimum as n varies, which is relatively high when n' is small, but decreases to small values for large values of the refractive index. At visible light wavelengths, where the refractive indices of glasses are in the 1.45–1.65 range, the improvement resulting from the introduction of a shell, in comparison with the uncorrected cavity, is modest. The minimum value of $\Delta^{(6)}$ is found to be $62\,Rp^6$, for $n' = 1.6$. A substantial improvement can be obtained, however, at ir wavelengths,* where the refractive indices of available materials can be as high as 4 (germanium). When the shell is made of germanium ($n' = 4$), the fifth-order aberration reaches a minimum $\Delta^{(6)} = 0.8Rp^6$, for a core refractive index $n = 3.7$. For $n = 3.3$ (gallium arsenide) the aberration is not substantially larger. It was verified, by calculating $U(p)$ as a function of p, that aberrations of order higher than the fifth are negligible in the range of Δ of interest. The maximum value of p for $n = 3.5$ is found to be 0.43, corresponding to an angle of 25°. For larger angles the ray still intersects the shell, but it misses the core. Figure 5 gives, for $n' = 4$, the required radii r, r' as functions of n. The acceptance factor is obtained by substituting the expression of the leading term $\Delta^{(6)}$, obtained from Eqs. (9c) and (26), in Eq. (14) and integrating with the same limits as in Sec. III.B.† One obtains at the resonant frequency ($\delta = 0$)

$$N = (R/\lambda)^{5/6}\mathfrak{F}_0^{-1/2}\mathfrak{N}, \tag{27}$$

where

$$\mathfrak{N} = (2\pi^3 10^{1/2}/3)\left[1 + \frac{R^5}{r'^5}\left(\frac{1}{n'^5} - 1\right) + \frac{R^5}{r^5} \times \left(\frac{1}{n^5} - \frac{1}{n'^5}\right)\right]^{-1/2}, \tag{28}$$

r/R and r'/R being obtained from the solutions of $\Delta^{(2)} = \Delta^{(4)} = 0$. $\mathfrak{N}$ is plotted in Fig. 5 as a function of n.

Taking the same numerical values as for the uncorrected cavity ($R = 10$ cm, $\lambda = 10\,\mu$m, $\mathfrak{F}_0 = 100$, $n = 4$) and $n' = 3.4$ one obtains $N = 19 \times 10^6$ which shows that an improvement by a factor of 5.5 results from the addition of a shell to the lens.

A modification of practical interest can be applied to any degenerate cavity consisting of concentric spheres. It consists of limiting the inner lens by a corner cube having its top at the cavity center, as shown in Fig. 6. This new configuration still meets the condition for degeneracy; it requires only one eighth of the volume of the refractive medium used in the full cavity. Figure 6 represents a specific configuration with a shell in germanium and a core in gallium arsenide. The refractive index of the core is high enough to provide total reflection on the corner cube faces. We also notice that antireflective coating is needed only outside the lens, the Fresnel reflection at the Ge–GaAs interface being less than 1%. The finesse of this cavity would presumably be limited by the bulk losses in germanium. In some applications, the losses can be overcome with the help of active media (CO_2 laser, for instance). In Fig. 7, a comparison is made of the refractive index laws for spherical degenerate cavities incorporating Luneburg lenses, spherical lenses, or optimum core and shell lenses.

IV. Cavities with Rotational Symmetry

We are considering in this chapter degenerate cavities which possess only optical rotational symmetry. In contrast to the case of spherical cavities, perfect imaging of the end mirrors is *not* a sufficient condition for low cavity aberrations. All six coefficients in the expansion of $\Delta^{(4)}$ must be considered, rather than the five aberration coefficients given in most textbooks (which refer to the imaging of a single plane).

In Sec.IV.A, we calculate the acceptance factor of confocal cavities on the basis of an expression of the wave aberration obtained by Connes.[5]

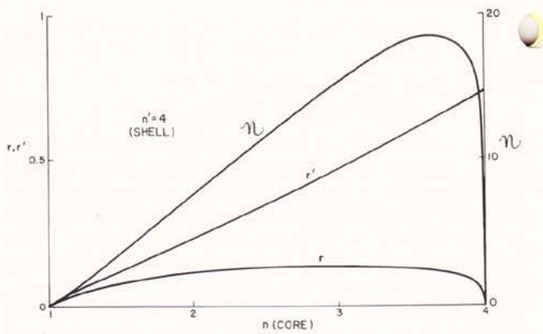

Fig. 5. When a high refractive index shell is added to the internal lens of the cavity shown in Fig. 3, the primary spherical aberration can be corrected. The required core and shell radii (r and r', respectively) are given in this figure as functions of the core refractive index (n), the shell refractive index being constant and equal to 4 (germanium). $\mathfrak{N}$ is proportional to the cavity acceptance factor, which is determined by the secondary spherical aberration. The mirror radius R is taken as unity.

* T. di Francia [J. Appl. Phys. **32**, 2051 (1961)] proposed a similar lens for the imaging of an object located at infinity.

† One uses the equality $\int_0^\infty du/(1 + u^6) = \pi/3$.

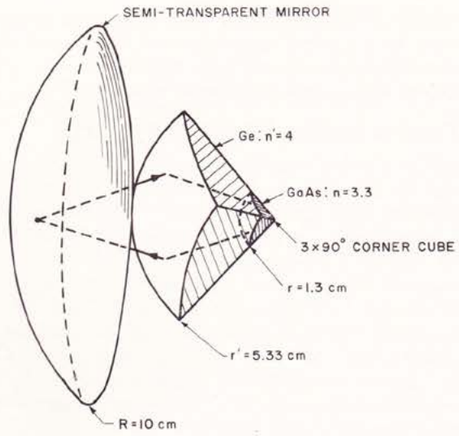

Fig. 6. This figure represents a corrected degenerate cavity of interest at ir wavelengths, based on the results of Fig. 5. Degeneracy is preserved when the internal lens is shaped as a corner cube.

A. Confocal Cavity

This cavity incorporates two spherical mirrors of radii R separated by an equal distance R.[9] Let us calculate the optical length of a quasiparaxial ray (defined in Sec. II.B) which intersects the end mirrors at radii ρ_1 and ρ_2, respectively, in meridional planes including an angle θ. One has

$$\Delta = 2(R'^2 + \rho_1^2 + \rho_2^2 + 2\rho_1\rho_2\cos\theta)^{1/2} + 2(R'^2 + \rho_1^2 + \rho_2^2 - 2\rho_1\rho_2\cos\theta)^{1/2}, \tag{29}$$

where

$$R' \equiv (R^2 - \rho_1^2)^{1/2} + (R^2 - \rho_2^2)^{1/2} - R.$$

Assuming that P_1, $P_2 \ll R$, one obtains

$$L + \Delta^{(4)} \simeq 4R - \rho_1^2\rho_2^2\cos 2\theta/R^3. \tag{30}$$

This result shows that, with the present choice of variables, a confocal cavity suffers only from astigmatism without field curvature.[5]

Examples of the error (in %) resulting from higher order terms ($m \geq 6$) for relatively large values of ρ_1 and ρ_2, obtained by ray tracing, are given in Table I.

Table I shows that the third-order approximation Eq. (30) provides a sufficient accuracy for the present problem.

Let us evaluate the acceptance factor of the confocal cavity by assuming that the stops, located at the end mirrors, have radii such that the wave aberration does not exceed $\lambda/\mathfrak{F}_0$. Because the cavity is only half-degenerate, incident beams have to be restricted to half the input aperture area and half the accepted solid angle. These considerations lead to

$$N \simeq (R/\lambda)\mathfrak{F}_0^{-1}. \tag{31}$$

For $R = 1$ m, $\lambda = 10\,\mu$m, $\mathfrak{F}_0 = 100$, one obtains $N \simeq 1000$.

B. Two-Lens Cavity

Let us consider now the two-lens degenerate cavity shown before in Fig. 1 and redrawn in Fig. 8, which incorporates two confocal lenses of equal focal length f between two plane end mirrors.

The wave aberration can be obtained by calculating the path length of a quasiparaxial ray defined by radii ρ_1 and ρ_2 at the input plane and at the central plane, respectively, and the angle θ between the two corresponding meridional planes. Let us first assume that the lenses can be replaced by thin planes introducing at a distance ρ from the axis an optical delay

$$V = -\rho^2/2f, \tag{32}$$

f being the focal length of the lenses. V is taken as independent of the incidence angle, to satisfy the general laws of optics. Equation (32) is a valid approximation for lenses of large refractive indices and radii, as we shall see in more detail later. With this approximation, one easily finds that

Table I. Error on Aberration

ρ_1/R	ρ_2/R	θ	$100[(\Delta - L)/\Delta^{(4)} - 1]$
0.01	0.051	78°	<0.07
0.1	0.1	0	−3.5
0.1	0.11	26°	−4.6

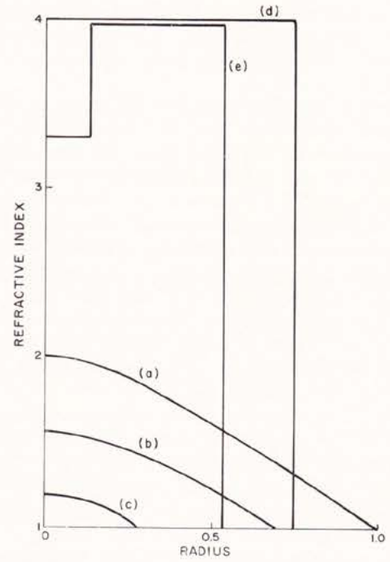

Fig. 7. This figure summarizes the various radial refractive index laws considered in Ref. 1 and in the present paper; (a) corresponds to the Maxwell fisheye medium $n(r) = 2(1 + r^2)^{-1}$, (b) and (c) correspond to Luneburg lenses calculated for the case where the object and the image occupy symmetrical positions, (d) is relative to a typical Pole's cavity (Fig. 3), and (e) is relative to the corrected version represented in Fig. 6.

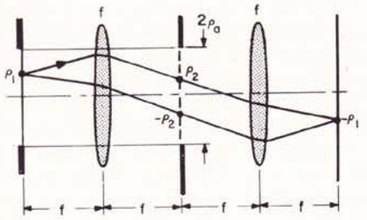

Fig. 8. Two-lens cavity incorporating stops at the input plane and at the central plane. For lenses with high refractive indices, primary aberrations can be corrected, in principle, with the help of two aspherical plates.

$$L + \Delta^{(4)} = 8f - (f/2)(\rho_1^4/f^4 + \rho_2^4/f^4). \quad (33)$$

Let us substitute now Eq. (33) into Eq. (14), the limits of integration being defined by two apertures of equal radius ρ_a, at the input plane and at the central plane. One obtains*

$$N = (\pi^3/4)(f/\lambda)\mathfrak{F}_0^{-1}[\tan^{-1}(\mathfrak{a} - \delta) + \tan^{-1}(\delta)], \quad (34)$$

where δ was defined before [Eq. (19)], and the aperture factor is

$$\mathfrak{a} = \mathfrak{F}_0\rho_a^4/\lambda f^3. \quad (35)$$

As an example, let us assume that $\lambda = 10$ μm, $f = 0.5$ m, and $\mathfrak{F}_0 = 100$. $\mathfrak{a} = 1$ corresponds to aperture radii $\rho_a = 1.05$ cm, and the maximum wave aberration is, in that case, equal to $\lambda/\mathfrak{F}_0$. The acceptance factor, at the peak of the response curve ($\delta = 0.5$), is from Eq. (34), $N = 3675$.

The form of the aberration Eq. (33) suggests that all third-order aberrations can be corrected by using aspherical plates at the input plane (to correct for the term $-\rho_1^4/2f^3$) and at the central plane (to correct for the term $-\rho_2^4/2f^3$). Equation (33), however, is valid only for high refractive index lenses. To avoid lengthy analytical calculations, ray tracing was used to evaluate the wave aberration for the case of symmetrical 5-mm thick germanium lenses ($n = 4$) and glass lenses ($n = 1.5$). The focal lengths f of the two lenses are taken as unity (1 m). The primary aberration coefficients, obtained by this method, are given in Table II, together with the result of Eq. (33). The terms $\rho_1^2\rho^2_3$ and $\rho_2^2\rho_3^2$ (distortion and coma) are always absent, as a result of the symmetry. Table II shows that the use of asphericities at the input mirror and at the central plane would not cancel exactly all third-order aberrations, but would, however, bring a substantial improvement in the case of germanium lenses.

The acceptance factors of cavities with nonplanar path shown in Fig. 3 of Ref. 1 are four times larger, for the same free spectral range, because two lenses only are encountered in a round trip, instead of four. The aberration terms are otherwise the same.

V. Cavities Lacking Rotational Symmetry

Cavities lacking rotational symmetry are strongly affected by aberrations, since the primary aberrations are, in that case, of second order. Ray tracing was used to evaluate the wave aberration of the internal mirror cavity, discussed in Ref. 1, Sec. III.B, which incorporates two internal spherical mirrors of equal radius R and two plane end mirrors.* This cavity clearly lacks rotational symmetry. The dimensions of this cavity were given in Eq. (12) of Ref. 1. The present results are given for incidence angles on the spherical mirrors equal to 45°. Ray tracing shows that the wave aberration dependance on x_0 and y_0 is

$$\Delta^{(3)}(x_0,y_0,0,0) = -0.5x_0^3R^{-2} + 4y_0^3R^{-2}. \quad (36)$$

A rough estimate of the acceptance factor can be derived from Eq. (36):

$$N \simeq (R/\lambda)^{2/5}\mathfrak{F}_0^{-4/5}. \quad (37)$$

If $R = 1$ m, $\lambda = 10$ μm, and $\mathfrak{F}_0 = 100$, one finds that $N \simeq 5$. This type of cavity, although attractive in some other respects, is consequently by far inferior to all the other cavities discussed before in this paper.

VI. Conclusions

The acceptance factor of degenerate optical cavities is primarily limited by geometrical optics aberrations. It was given for a number of cavities of interest, including the well-known plane parallel Fabry-Perot and the confocal cavity. Typical values obtained for the acceptance factors of these cavities are listed in Table III. The round trip path lengths of the cavities are, respectively, 0.4 m and 4 m for the cavities with spherical and rotational symmetries (it would be impractical to make large spherical lenses). The values given for the resolution are based on the assumption of no losses or defects in the cavities, and mirror reflectivities of 97%.

Table II. Primary Aberration Coefficients

n	$\Delta^{(4)}$	($\rho_3^2 \equiv \rho_1\rho_2\cos\theta$)
∞	$-0.5\ \rho_1^4 - 0.5\ \rho_2^4$	[Eq. 33)]
100	$-0.505\ \rho_1^4 - 0.505\ \rho_2^4 - 0.01\ \rho_3^4 - 0.01\ \rho_1^2\rho_2^2$	
4	$-0.66\ \rho_1^4 - 0.66\ \rho_2^4 - 0.138\ \rho_3^4 - 0.32\ \rho_1^2\rho_2^2$	
1.5	$-1.66\ \rho_1^4 - 1.66\ \rho_2^4 - 3.32\ \rho_3^4 - 2.33\ \rho_1^2\rho_2^2$	

* To simplify the integration, the square limit in the ρ_1^2, ρ_2^2 plane is replaced by a circular limit of radius ρ_a^2. This introduces only a small error.

* Experiments made at $\lambda = 0.6328$ μm with $R = 3$ m confirmed that this cavity is degenerate, to first order.

Table III. Typical Values Obtained for Cavity Acceptance Factors

Name of the cavity (as used in the text)	Typical acceptance factor $\simeq$ étendue/λ^2 N	Typical resolution $L\mathfrak{F}/\lambda$	Comments
Single mode cavity (Sec. II)	1	4×10^7	Used with coherent sources. Requires mode matching
Internal mirror cavity (Sec. V)	5	4×10^7	Does not incorporate lenses. Lacks rotational symmetry
Plane parallel Fabry-Perot. 1-cm spacing, 10-cm² area (Sec. III.A)	148	10^5	Widely used because of its simplicity. Narrow acceptance angle
Confocal cavity (Sec. IV.A)	1000	4×10^7	Does not incorporate lenses. Alignment not critical
Two-lens cavity (Sec. IV.B)	3675	4×10^7	Flexible arrangement. Primary aberrations can be corrected to some extent
Concentric cavity (Sec. III.B)	3.8×10^6	2×10^6	Spherical symmetry
Corrected concentric cavity (Sec. III.C)	19×10^6	2×10^6	Spherical symmetry. Corrected for primary aberrations (ir wavelengths)
Maxwell fisheye cavity (Sec. II.A)	10^9	3×10^6	Spherical symmetry. Aberration free. Not feasible at the present time

Table III clearly shows that the acceptance factor of cavities with spherical symmetry, whether or not they are corrected, is larger, by orders of magnitude, than the acceptance factor of cavities which possess only rotational symmetry. The lenses required in spherical cavities, however, are bulky, and consequently lossy, particularly at ir wavelengths. It may also be difficult to make full use of the wide acceptance angle of these cavities, i.e., to match their acceptance angle to the radiation angle of commonly encountered sources, which usually do not extend over the whole half-space.

The main difficulty in the fabrication of degenerate optical cavities is that every ray keeps passing through each optical element at the same point a large number of times, roughly equal to the finesse $\mathfrak{F}_0$. As a consequence, the phase errors (lense defects as well as aberrations) add up, and create large total phase distortions. The future use of degenerate optical cavities consequently rests on improvements in lens polishing, alignment, and over-all mechanical accuracy, which have to be better by orders of magnitude than the ones required for conventional optical instruments.

The author expresses his thanks to D. C. Hogg and T. S. Chu for useful discussions. The numerical calculations relative to the symmetrical Luneburg lenses were made by C. L. Beattie.

References

1. J. A. Arnaud, Appl. Opt. **8**, 189 (1969).

2. J. A. Arnaud, Appl. Opt. **8**, 1909 (1969). Notice obvious misprints in Eqs. (13c), (18), and (23). Reference (20) was intended to refer to the present paper.

3. R. K. Luneburg, *Mathematical Theory of Optics* (University of California Press, Los Angeles, 1964).

4. R. A. Myers and R. V. Pole, IBM J. Res. Dev. **11**, 502 (1967).

5. P. Connes, Rev. Opt. **35**, 1 (1956).

6. R. V. Pole, J. Opt. Soc. Amer. **55**, 254 (1965).

7. A. Yariv and H. Kogelnik, Proc. IEEE **52**, 165 (1964).

8. See, for instance, W. Brouwer and A. Walther, in *Advanced Optical Techniques*, A. C. S. Van Heel, Ed. (North-Holland Publishing Company, Amsterdam, 1961), Chaps. 16, 17.

9. M. Hercher, Appl. Opt. **7**, 951 (1968). Notice that the expression for the wave aberration of a confocal resonator given in this paper has an incorrect sign. For further information on confocal resonators, see D. J. Bradley and C. J. Mitchell, Phil. Trans. Roy. Soc. London, **A263**, 209 (1968).

10. J. V. Ramsay, Appl. Opt. **8**, 569 (1969).

11. M. Herzberger, *Modern Geometrical Optics* (Interscience Publishers, Inc., New York, 1958). For a detailed analysis of the imaging by glass spheres, see A. Walther, "Optical Applications of Solid Glass Spheres," thesis, University of Delft, 1959.